itative MO treatment proposed by Bursten,[37] which compares the electronic properties of model complexes having two cis CO ligands with those having two trans CO ligands.[39] This scheme is shown in Figure 7; the two energy level diagrams represent the d_π orbitals for the isomers of $M(CO)_2L_4$, where M is a metal with six d electrons and L is a ligand with poorer π-acceptor ability than CO. This scheme is in agreement with the experimentally observed properties of $Mo(CO)_2(CNR)_2(PR'_3)_2$, that is, the trans CO isomers are easier to oxidize because the electron is removed from an orbital of higher energy than that of the cis isomer HOMO. The HOMO of the trans isomer has no stabilization from interaction with CO ligands, while all the orbitals of the cis isomer are stabilized to some extent by interaction with CO. The preference for one geometry over another depending on oxidation state is similarly explained: the cis isomer is stabilized the maximum amount by having 18 electrons, while the trans isomer is equally stable with 16, 17, or 18 electrons. The rapid isomerization to the trans isomer when an electron is removed from the cis isomer is nicely explained in this manner.[40]

Acknowledgment. Support of this research by the National Science Foundation (Grants CHE82-06117 and CHE85-06702) is gratefully acknowledged.

Supplementary Material Available: Tables giving homogeneous chemical rate constants for the cis-trans isomerization of $Mo(CO)_2(CNR)_2(PR'_3)_2$ (Table SI), IR spectral data for $[Mo(CO)_2(CNR)_2(PR'_3)]^+$ (Table SII), and electronic absorption spectral data for $Mo(CO)_2(CNR)_2(PR'_3)_2$ (Table SIII) and figures showing cyclic voltammograms of $Mo(CO)_2(CN(t\text{-}Bu_3Ph))_2(P\text{-}n\text{-}Pr_3)_2$ (Figure S1), the $^{31}P\{^1H\}$ NMR spectrum of $Mo(CO)_2(CNxylyl)_2(PEt_2Ph)_2$ (Figure S2), and the ESR spectrum of $[Mo(CO)_2(CN(t\text{-}Bu_3Ph))_2(P\text{-}n\text{-}Pr_3)_2]^+$ (Figure S3) (8 pages). Ordering information is given on any current masthead page.

(39) EHMO calculations on the model complexes $[Mo(CO)_2(PH_3)_4]^{+/0}$ show that the cis form is favored in 18-electron systems and the trans form in 17-electron systems; see: Mingos, M. P. *J. Organomet. Chem.* **1979**, *179*, C29.

(40) Measurements carried out on the tungsten complex $W(CO)_2(CNxylyl)_2(P\text{-}n\text{-}Pr_3)_2$ show that it behaves in a similar fashion to its molybdenum analogues; consequently a discussion of its properties is not given in the text. Its spectroscopic and electrochemical properties are summarized in Tables I-IV and SI-SIII. The complex was prepared as an orange powder by the reaction of $(\eta^3\text{-}C_3H_5)WCl(CO)_2(CNxylyl)_2$ with $P\text{-}n\text{-}Pr_3$ in CH_2Cl_2 solution (see procedure B.1. in the Experimental Section) and recrystallized from CH_2Cl_2/MeOH.

Contribution from the Department of Chemistry,
Michigan State University, East Lansing, Michigan 48824

NMR and Potentiometric Studies of Lithium Salts in 1-Butylpyridinium Chloride-Aluminum(III) Chloride Molten Systems

Rick R. Rhinebarger, John W. Rovang, and Alexander I. Popov*

Received March 20, 1986

Lithium-7 NMR and potentiometric measurements have been used to identify and characterize lithium chloro complexes of the lithium ion in the *n*-butylpyridinium chloride-aluminum chloride ($AlCl_3$-(BP)Cl) ambient temperature molten salt media. Concentration-dependent ^7Li chemical shift data have been fitted to a two-site fast-exchange model that assumes an equilibrium between the $LiCl_2^-$ monomer and the $Li_2Cl_4^{2-}$ dimer species ($\log K_d = 2.82$ (± 0.39) M^{-1}, K_d = dimerization constant). Potentiometric measurements on LiCl and $LiClO_4$ solutions in basic melt (45 mol % $AlCl_3$) confirm that two chloride ions are associated with each lithium ion.

Introduction

The $AlCl_3$-*n*-butylpyridinium chloride ambient temperature molten salt system, first described by Osteryoung et al.,[1] has been shown to be a highly versatile anhydrous medium for many chemical applications and, in particular, for studies of various complexation equilibria.[2-6] Our interest in this system is focused primarily upon the interaction of alkali-metal cations with the components of these media as well as on the influence of those "nonaqueous solvents" on the formation of macrocyclic complexes of the alkali-metal ions.[7,8]

The purpose of this work was to characterize in greater detail the environment of the lithium ion in basic (mole fraction $AlCl_3 < 0.50$) and acidic (mole fraction of $AlCl_3 > 0.50$) melts, to identify various lithium species (chloro complexes and crown ether complexes), and to study their interactions in the melt. Lithium-7 chemical shifts, spin-lattice (T_1) relaxation measurements, and potentiometric titration methods have been used to obtain this information.

Experimental Section

n-Butylpyridinium chloride was prepared by the method of Osteryoung et al.[1] The salt was recrystallized twice from an acetonitrile-ethyl acetate mixture and dried under vacuum; it was then stored in vacuum-sealed ampules until used. Aluminum(III) chloride (Fluka) was distilled under vacuum in the presence of aluminum wire (Alfa). Lithium chloride and lithium bromide (Fisher), lithium nitrate (Mallinckrodt), and lithium perchlorate and lithium hexafluoroarsenate (Alfa) were dried for 3 days at 100 °C.

Preparation of all melts and solutions was carried out in a drybox under an inert-gas atmosphere with a combined $H_2O + O_2$ level of less than 10 ppm. All NMR samples were contained in 5 mm (Wilmad) vacuum-sealed NMR tubes.

Lithium-7 NMR measurements were made on a Bruker WH-180 spectrometer at the field of 42.28 kG and at a resonance frequency of 69.951 MHz. Except where otherwise indicated, NMR spectra were obtained at 40 (±1) °C. The instrument was locked on the deuterium signal of the primary external reference (0.015 M LiCl in D_2O) for all samples where the overlap with the ^7Li signal of the reference did not occur. Otherwise, a secondary reference (0.015 M LiCl in pyridine) was used, and spectra were obtained without lock. Chemical shifts (except those in acidic melt solutions) are corrected for differences in magnetic susceptibility between the melt and water. The uncertainties in chemical shift values are ±0.02 ppm. Downfield (paramagnetic) shifts are indicated as *positive*. The magnetic susceptibility of the 45:55 mol % $AlCl_3$-(BP)Cl melt was determined at 40 °C by using an SHE Corp. 800

(1) Gale, R. J.; Gilbert, B.; Osteryoung, R. A. *Inorg. Chem.* **1978**, *17*, 2728. Gale, R. J.; Osteryoung, R. A. *Inorg. Chem.* **1979**, *18*, 1603.
(2) Pickup, P. G.; Osteryoung, R. A. *J. Am. Chem. Soc.* **1984**, *106*, 2294.
(3) Hussey, C. L.; King, L. A.; Wilkes, J. S. *J. Electroanal. Chem. Interfacial Electrochem.* **1979**, *102*, 321.
(4) Schoebrechts, J. P.; Gilbert, B. P.; Duyckaerts, G. *J. Electroanal. Chem. Interfacial Electrochem.* **1983**, *145*, 127.
(5) Fannin, A. A.; King, L. A.; Levisky, J. A.; Wilkes, J. S. *J. Phys. Chem.* **1984**, *88*, 2609.
(6) Lipsztajn, M.; Osteryoung, R. A. *Inorg. Chem.* **1985**, *24*, 716.
(7) Taulelle, F.; Popov, A. I. *Polyhedron*, **1983**, *2*, 889.
(8) Rhinebarger, R. R.; Rovang, J. W.; Popov, A. I. *Inorg. Chem.* **1984**, *23*, 2557.

0020-1669/86/1325-4430$01.50/0

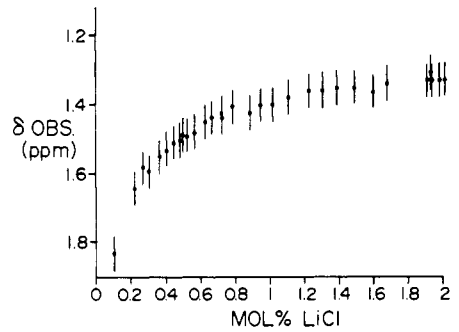

Figure 1. Concentration dependence of the ^{7}Li chemical shift of LiCl solutions in the basic $AlCl_3$–BPCl melt at 40 °C.

Series SQUID susceptometer ($\chi = -0.761 \times 10^{-6}$).

Spin–lattice relaxation measurements were made by using the fast inversion–recovery Fourier transform (FIRFT) method of Canet et al.[9] Lithium-7 chemical shift and relaxation data reduction were performed on a CDC 6500 computer system; the nonlinear-least-squares program KINFIT[10] was used to treat the data.

Silver electrodes were prepared by successively rinsing silver wire (Aldrich Gold Label; 99.99%) with concentrated nitric acid, with deionized water, and with acetone, followed by air-drying. Potentiometric titrations were carried out in a 25 × 40 mm Pyrex weighing bottle containing a Teflon-coated stirring bar. The reference compartment was constructed from 0.5-in. Pyrex glass tubing with fine-porosity Pyrex fritted glass disks sealed into the tube constrictions. The fritted glass disks were conditioned prior to use by soaking them in a basic melt solution of silver acetate ($X_{Ag} = 2.0 \times 10^{-5}$). An equivalent amount of the silver acetate was added to the basic melt. Cell potentials were measured with a Markson Science Electro Mark Analyzer multipurpose meter in the millivolt mode to ±1 mV. All titrations were performed at 35 ± 2 °C. Titrants were added through precalibrated disposable glass pipet tips by using a Brinkmann Eppendorf digital pipettor.

Results and Discussion

(I) NMR Measurements. As we reported previously,[8] basic (45:55 mol % $AlCl_3$:(BP)Cl) melt solutions of LiCl exhibit a single, population-averaged signal that is downfield from the external references. With 1.0 mol % LiCl and at 40 °C, a chemical shift of +1.56 (±0.02) ppm with a line width of 25 (±1) Hz was obtained. Between 0.1 and 2 mol % LiCl (the approximate solubility limit for LiCl in basic melt at 40 °C), a substantial concentration dependence of the chemical shift was observed (Figure 1). In addition, from 35 to 90 °C, a small ($\Delta\delta/\Delta T$ = +0.003 ppm/°C) but consistent temperature dependence was observed for the ^{7}Li signal of 1.0 mol % solution of LiCl. As the temperature was increased through this range, the line width of the signal decreased from 25 to 8 Hz, very probably due to the decrease in viscosity.

In addition to LiCl, other lithium salts (LiSCN, LiBr, $LiNO_3$, $LiClO_4$, and $LiAsF_6$) were found to be soluble in the basic melt at 40 °C. However, in all cases these solubilities were less than that of the LiCl and varied in the range $1.5 \leq S \leq 2.0$ mol %. Within experimental error, the chemical shifts observed for 1.0 mol % basic melt solutions of the thiocyanate, bromide, nitrate, perchlorate, and thiocyanate salts were identical.

In the acidic melt (67 mol % $AlCl_3$) at 40 °C, where LiCl is soluble up to ~9 mol %, the ^{7}Li NMR signal was observed at $\delta = -1.14$ (±0.02) ppm ($W_{1/2} = 2$ (±1) Hz). The chemical shift and the line width of this signal were found to be insensitive to the lithium ion concentration, to the nature of the anion, or to the temperature (35–90 °C).

The marked concentration dependence of ^{7}Li chemical shift suggested to us that more than one lithium species exists in basic melt. Several solution equilibrium models were evaluated by computer-fitting of these data. The model that gives by far the best fit for the observed behavior of the chemical shift assumes the association of the $LiCl_2^-$ species[8] to form the $Li_2Cl_4^{2-}$ dimer in a fast two-site exchange condition. In this model the association

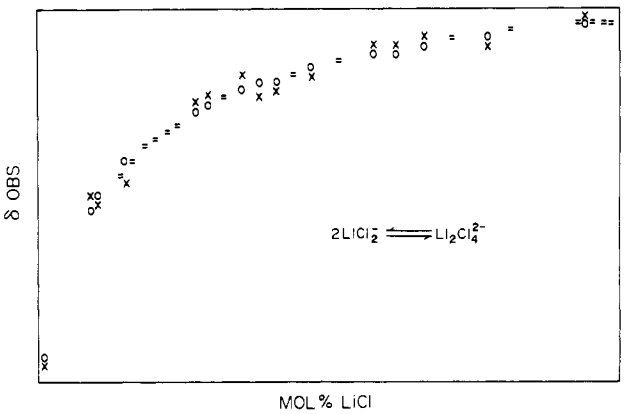

Figure 2. Least-squares fitting of the ^{7}Li resonance vs. mol % LiCl to the dimerization model: (×) experimental points; (○) calculated points; (=) coincidence of the experimental and the calculated points within the resolution of the plot.

Table I. Lithium-7 T_1 Relaxation Times for Lithium Salts in the $AlCl_3$–(BP)Cl System at 25 and 40 °C[a]

sample	25 °C	40 °C
1.0 mol % LiCl	0.046 ± 0.002	0.043 ± 0.002
2.0 mol % LiCl	0.063 ± 0.004	0.061 ± 0.003[b]
1.0 mol % LiBr	0.050 ± 0.003	0.049 ± 0.005[b]
1.0 mol % $LiClO_4$	0.051 ± 0.003	0.048 ± 0.002
1.0 mol % $LiAsF_6$	0.050 ± 0.003	0.052 ± 0.003
1.0 mol % $LiNO_3$	0.041 ± 0.002	0.039 ± 0.008[b]
1.0 mol % LiCl	1.10 ± 0.27	1.52 ± 0.08

[a] The first six measurements were carried out in basic melt (45 mol % to $AlCl_3$); the last was carried out in an acidic melt (67 mol % $AlCl_3$). [b] Single experiments; all other values are the averages of two experiments.

constant and the limiting chemical shifts of the two species are the adjustable parameters.

A plot of the calculated and experimental data is shown in Figure 2. Other models, which assumed interactions of $LiCl_2^-$ with $AlCl_4^-$, or with BP^+ ions, or the dissociation of $LiCl_2^-$ to form Li^+Cl^- ion pairs or free lithium ion etc., do not fit the experimental data. In addition, no further improvement in the fit was obtained by including the tetramer, as well as the dimer species. Of course the dimerization of lithium salts in nonaqueous solution has been amply documented by numerous authors.[11,12]

A log K_d (dimerization constant) value of 2.82 (±0.39) for the dimerization reactions. Although the dimerization constant that we have obtained seems to be rather large by comparison with those obtained in nonaqueous solvents, one must view this result within the context of an ionic liquid where strong ionic associations are predominant.

At this time we do not have sufficient information to speculate on the structure of the dimer. It should be noted, however, that the lithium ion has the tendency to assume nearly tetrahedral four-coordination geometries in molten salts, as was indicated in a recent molecular dynamics study of the LiCl–KCl eutectic melt by Okada et al.[13]

Lithium-7 spin–lattice relaxation times were obtained at 25 and 40 °C for 1.0 mol % solutions of LiCl, LiBr, $LiClO_4$, $LiAsF_6$, and $LiNO_3$ in 45–55 mol % $AlCl_3$–(BP)Cl melt. In addition, T_1 relaxation times were obtained for 2.0 mol % LiCl in the above melt and 1.0 mol % LiCl in 67–33 mol % $AlCl_3$–(BP)Cl melt. These results are summarized in Table I. At 1.0 mol % of the lithium salt, T_1 values were independent of the counterion; however, nearly a 50% increased in T_1 was obtained when the con-

(9) Canet, D.; Levy, G. C.; Peat, I. R. *J. Magn. Reson.* **1975**, *18*, 199.
(10) Dye, J. L.; Nicely, J. A. *J. Chem. Educ.* **1971**, *48*, 443.
(11) Harada, Y.; Salomon, M.; Petrucci, S. *J. Phys. Chem.* **1985**, *89*, 2006 and references quoted therein.
(12) Chabanel, M.; Wang, Z. *Can. J. Chem.* **1984**, *62*, 2320 and references quoted therein.
(13) Okada, I.; Okano, M.; Ohtaki, H.; Takagi, R. *Chem. Phys. Lett.* **1983**, *100*, 436.

centration of LiCl was doubled. Within the experiment error, an increase in temperature from 25 to 40 °C had no effect on T_1 values for all lithium salts in 45 mol % $AlCl_3$ melt. In the acidic melt, the T_1 was longer by nearly 2 orders of magnitude and was temperature-dependent.

The independence of the ^7Li chemical shifts and T_1 relaxation times in basic melt of the nature of the anion indicates that in this medium the nearest-neighbor coordination shell of the lithium ion is composed of chloride ions, irrespective of the anion of the original salt.

II. Potentiometric Measurements. In previous potentiometric studies of metal ion chloro complexes in the $AlCl_3$–(BP)Cl system, metal indicator electrodes, responsive to changes in metal ion activity, have been used with aluminum reference electrodes (dipping in 2:1 $AlCl_3$–(BP)Cl melt).[14] However, this configuration is restricted to studies of M/M^{n+} couples which are electrochemically reversible. In devising a potentiometric technique for the study of lithium chloro complexes in basic $AlCl_3$–(BP)Cl melt, it was anticipated that an irreversible reaction similar to that observed by Gale and Osteryoung[15] for aluminum in basic melt would be likely to occur if a Li/Li^+ couple was employed.

It has been pointed out by Plambeck[16] that the Ag/Ag^+ electrode is quite suitable as a standard reference electrode in molten salts; in addition, a silver indicator electrode can also be used to monitor the chloride ion activity in basic melts. Laher and Hussey[17] have shown that the Ag^+ ion forms very stable chloro complexes in the basic $AlCl_3$–(BP)Cl melt and that in dilute Ag^+ solutions more than 90% of the total silver ion is in the form of the $AgCl_4^{3-}$ complex.

The following concentration cell, with silver reference and indicator electrodes, was used to determine the coordination number of the lithium ion in basic melt:

$$\mathrm{Ag} \left| \begin{array}{c} \mathrm{Ag}^+,\ \mathrm{BASIC\ MELT} \\ (\mathrm{pCl} = 1.000) \end{array} \right| \begin{array}{c} \mathrm{GLASS} \\ \mathrm{FRIT} \end{array} \left| \mathrm{BASIC\ MELT},\ \mathrm{Ag}^+ \right| \mathrm{Ag}$$

where the right electrode (E_r) is the indicator electrode. The left-hand reference cell compartment contained melt that was 45.00 mol % in $AlCl_3$, with a small amount of silver acetate ($X_{Ag(I)} = 2 \times 10^{-5}$).

For the equilibrium

$$Ag^+ + 4Cl^- \overset{\beta_4}{\rightleftharpoons} AgCl_4^{3-}$$

we have

$$\beta_4 = X_{AgCl_4^{3-}}/X_{Ag^+}X_{Cl^-}{}^4 \qquad (1)$$

where β_4 is the overall formation constant of the $AgCl_4^{3-}$ complex ($=1.6 \times 10^{23}$ [17]) in mole fraction units. We assumed the Temkin ideal solution model for molten salts,[18] where the activity of an ion in solution is taken to be equal to its mole fraction ($a_i = X_i$). Assuming that the concentrations of the $AgCl_2^-$ and $AgCl_3^{2-}$ complexes may be neglected,[17] we get

$$X_{Ag(I)} = X_{Ag^+} + X_{AgCl_4^{3-}} \qquad (2)$$

Combination of (1) and (2) gives

$$X_{Ag^+} = X_{Ag(I)}/(1 + \beta_4 X_{Cl^-}{}^4) \qquad (3)$$

The potential of the silver indicator electrode is given by

$$E_r = E^{\circ\prime}{}_{Ag/Ag(I)} + \frac{RT}{F} \ln X_{Ag^+} \qquad (4)$$

where $E^{\circ\prime}{}_{Ag/Ag(I)}$ is the apparent standard potential of the Ag/Ag^+ couple. Substituting (3) into (4) and assuming that $1 << \beta_4 X_{Cl^-}{}^4$, we obtain

$$E_r = E^{\circ\prime}{}_{Ag/Ag(I)} + \frac{RT}{F} \ln \frac{X_{Ag(I)}}{\beta_4 X_{Cl^-}} \qquad (5)$$

The above approximation is justified, since X_{Cl^-} in 45.00 mol % $AlCl_3$ melt is 0.1000 and $\beta_4 X_{Cl^-}{}^4$ is $\sim 10^{19}$.

Regrouping terms and defining $pCl \equiv -\log X_{Cl^-}$, we get

$$E_r = E^{\circ\prime}{}_{Ag/Ag^+} + \frac{RT}{F} \ln \frac{X_{Ag}{}^{total}}{\beta_4} + \frac{2.303(4RT)pCl_r}{F} \qquad (6)$$

After a similar derivation for the potential of the reference silver electrode (E_1), it can be shown that

$$E_{cell} = E_{right} - E_{left} = \frac{2.303(4RT)}{F}(pCl_r - pCl_{ref}) \qquad (7)$$

Thus, changes in the chloride ion activity in the working compartment are readily observed by the measurement of the variation of the cell potential.

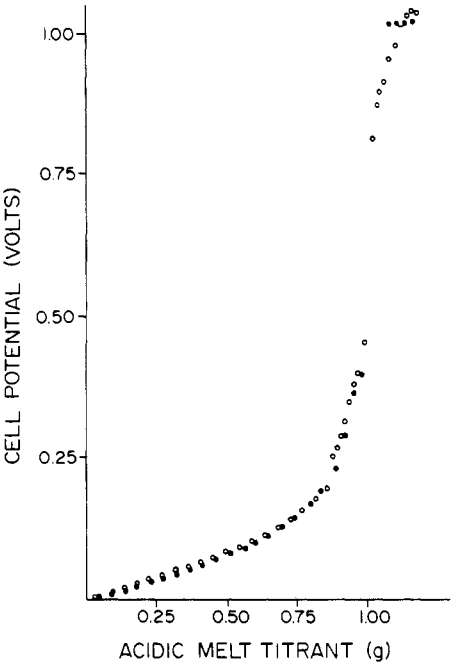

Figure 3. Titration curve of the 45–55 mol % $AlCl_3$–BPCl melt with the acidic melt. Open and closed circles indicate duplicate runs. The uncertainties in the amount of the titrant and in the cell potential are smaller than the circle size.

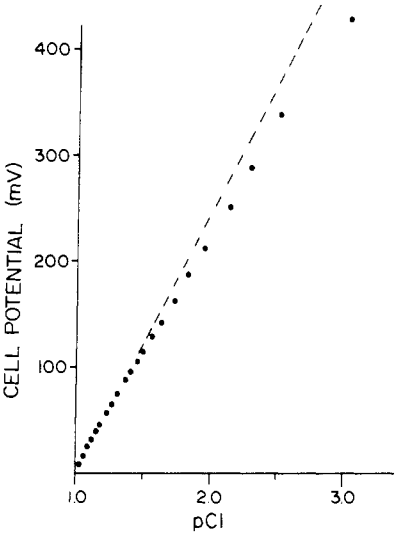

Figure 4. Variation of the cell potential with pCl.

(14) Chum, H. L.; Osteryoung, R. A. In *Ionic Liquids*; Inman, D., Lovering, D. G., Eds.; Plenum: New York, 1981.
(15) Gale, R. J.; Osteryoung, R. A. *J. Electrochem. Soc.* **1981**, *127*, 2167.
(16) Plambeck, J. A. *Proc.—Electrochem. Soc.* **1984**, 707.
(17) Laher, T. M.; Hussey, C. L. *Inorg. Chem.* **1983**, *22*, 1279.
(18) Temkin, M. *Acta Physicochim. URSS* **1945**, *20*, 411.

The working curves obtained in the potentiometric titration of 45.00 mol % $AlCl_3$ melt with acidic melt titrant at 35 °C are shown in Figure 3. In addition to its convenience, the volumetric addition method gave potentials that were both stable (±0.001 V) and reproducible (~±0.010 V) throughout most of the basic side of the titration curves. Cell potentials stabilized within 1 min of the addition of an aliquot of titrant that was 65.51 mol % in $AlCl_3$. Corrected values of X_{Cl^-} at each point in the titrations were then calculated. A plot of E_{cell} vs. the corrected pCl values is given in Figure 4. A least-squares fit of the first ten data points to eq 8 yielded a slope of 0.2435 V (theoretical slope at 35 °C = 0.2446 V).

The titration curves for the titration of the basic melt solutions of LiCl (0.977 mol %) and $LiClO_4$ (0.960 mol %) with 65.51 mol % $AlCl_3$ melt are shown in Figure 5. A finely dispersed precipitate (assumed to be LiCl) was observed in the course of each titration; in addition, the curve for the titration of the $LiClO_4$ solution was displaced to higher potentials (higher pCl) vs. that for the LiCl solution. It should be noted that both curves also start at slightly positive (~30–40 mV) cell potentials compared to those shown in Figure 3.

In the titrations of dilute LiCl and $LiClO_4$ basic melt solutions with the acidic melt, excess chloride ions (beyond that required to form the lithium chloro complexes) react with the titrant

$$Cl^- + Al_2Cl_7^- \rightleftharpoons 2AlCl_4^-$$

At the onset of precipitate formation, most of the chloride ion from the melt is exhausted, and chloride ion from the lithium chloro complex is consumed

$$LiCl_x^{1-x} + (x-1)Al_2Cl_7^- \rightleftharpoons LiCl(s) + 2(x-1)AlCl_4^-$$

As more titrant is added the precipitate begins to redissolve

$$LiCl(s) + Al_2Cl_7^- \rightleftharpoons Li^+ + 2AlCl_4^-$$

and the melt solution becomes clear at the equivalence point, signifying that the chloride ion from all three sources (melt, lithium chloro complex, and LiCl) has reacted. Thus, the number of moles of $Al_2Cl_7^-$ (n_t) required from the onset of precipitation to the equivalence point of the titration is given by

$$n_t = n_f + (x-1)n_c + n_{Li^+} \quad (8)$$

where n_f is the residual free chloride ion from the melt at the precipitation point, n_c is the number of moles of the lithium chloro complex $LiCl_x$, and n_{Li^+} is the total number of moles of LiCl added to the melt. Assuming that in the melt all of LiCl is in the form of the chloro complex, we have

$$n_c = n_{Li^+} \quad (9)$$

and

$$n_t = n_f + xn_{Li^+} \quad (10)$$

or

$$x = (n_t - n_f)/n_{Li^+} \quad (11)$$

For the titration of the $LiClO_4$ solution eq 8 becomes

$$n_t = n_f + (x-1)n_c \quad (12)$$

where x is given by

$$x = [(n_t - n_f)/n_c] + 1 \quad (13)$$

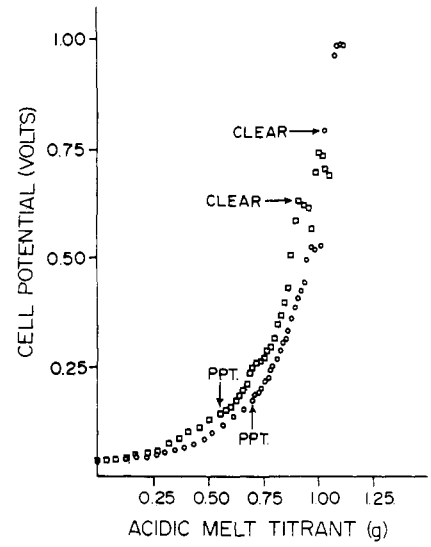

Figure 5. Titration curves for the titration of 0.977 mol % LiCl (○) and of 0.960 mol % $LiClO_4$ (□) with the acidic melt. Uncertainties in the abscissa and in the ordinate values are smaller than the size of the circle or of the square.

Table II. Results of Potentiometric Measurements and the Calculated Value of the Cl^-:Li^+ Ratio in the $LiCl_x$ Complex

	mol			mol	
	0.977 LiCl	0.960 $LiClO_4$		0.977 LiCl	0.960 $LiClO_4$
n_p	6.33×10^{-4}	6.59×10^{-4}	n_t[a]	2.43×10^{-2}	1.91×10^{-2}
n_f	2.21×10^{-4}	4.84×10^{-4}	x	2.2	2.0
n_c	1.91×10^{-4}	1.70×10^{-4}			

[a] Definitions of symbols are given in the text.

The cell potentials at which the precipitates are first observed are 175 mV for LiCl and 140 mV for $LiClO_4$, respectively; these potentials correspond to pCl values of 1.780 and 1.615, respectively. Thus, values for n_t are determined from the expression

$$n_t = n_p x_{Cl^-} \quad (14)$$

where n_p is the total number of moles in the melt at the point of precipitation. The results of these calculations for the LiCl and $LiClO_4$ titrations are given in Table II. The stoichiometric ratio of two chloride ions per lithium ion in the basic melt solution is confirmed. The fact that $x = 2$ for the $LiClO_4$ solution is further evidence that anions other than the chloride ion do not interact appreciably with the lithium ion in this medium.

Acknowledgment. The authors gratefully acknowledge the support of this work by National Science Foundation Grant CHE-8515474.

Registry No. LiCl, 7447-41-8; $AlCl_3$, 7446-70-0; butylpyridinium chloride, 1124-64-7.